Proceedings of International Symposium on Bond Behaviour of FRP in Structures (BBFS 2005)
Chen and Teng (eds)

SIZE EFFECT OF SHEAR CONTRIBUTION OF EXTERNALLY BONDED FRP U-JACKETS FOR RC BEAMS

Z. Qu[1,2] , X. Z. Lu[1,2], L. P. Ye[1,2]
1 Department of Civil Engineering, Tsinghua University, Beijing, China, 100084, China
2 Key Laboratory of Structural Engineering and Vibration of China Education Ministry,
Email: qz@mails.tsinghua.edu.cn; luxinzheng@263.net; ylp@tsinghua.edu.cn

ABSTRACT

It is well known that size effect exists in the shear strength of RC beams. Larger beams have a smaller nominal maximum shear strength. The size effect in RC beams shear strengthened with FRP has not been considered in existing predictive models. In these strengthened beams, the size effect may exist in the shear contributions of both RC beams and FRP. To better understand the shear strengthening and its corresponding size effect, a series of geometrically similar concrete beams strengthened with CFRP U-jackets were designed and tested in this study. The total shear strength of a strengthened RC beam is considered to consist of three components which are the shear contribution of the RC beam, and the direct and indirect shear contributions of the FRP. The direct shear contribution of FRP is obtained in this study with careful experimental measurements. An improved predictive model is proposed, which can obviously remove the size effect on direct FRP shear contribution. More studies are needed to quantify the indirect FRP shear contribution.

KEYWORDS

FRP, RC beams, shear strength, experiment, size effect.

INTRODUCTION

Extensive research has shown that size effect exists in the shear strength of RC beams without stirrups, which means that larger beams have smaller nominal shear strength. Fracture mechanics has been proved to be a powerful tool to solve the size effect problem. Bazant (1984) proposed a size effect theory considering stress redistribution and fracture energy release which was proved to be reasonable by an experimental study (Bazant 1991). Walraven and Lehwalter (1994) extended the application of Bazant's size effect theory to short beams with shear reinforcement and observed significant size effect on the shear strengths in their tests.

The wide use of FRP strengthening in civil engineering during the last decade has brought new problems to size effect. A lot research has been devoted to the shear strength of FRP strengthened RC beams but few considered size effect. Most existing models for predicting the shear contribution of FRP sheets adopted a superposition method, which assumes that the shear strength of an FRP strengthened RC beam is the sum of two components: the RC contribution and the FRP contribution. The RC contribution is considered to be the same as the shear strength of the RC beam without strengthening, whilst the FRP contribution is estimated with a sectional method whose generalized equation is shown in Eq.1.

$$V_f = \frac{A_f \varepsilon_{fe} E_f \left(\cot\theta + \cot\beta\right)\sin\beta \cdot h_{fe}}{s_f} \tag{1}$$

where V_f is the shear contribution of FRP sheets;

A_f is the sectional area of FRP sheets within a distance of s_f;

E_f is the Young's modulus of FRP sheets;

s_f is the central spacing of FRP sheets;

θ and β are the inclination angles of the diagonal crack and FRP sheets respectively, relative to the longitudinal axis of the beam;

h_{fe} is the effective height of FRP sheets;

ε_{fe} is the effective strain of FRP sheets, which is the key parameter of this kind of model.

Some of these models such as Chen and Teng (2003a, b) and Lu (2004) give satisfying predictions of FRP contributions with superposition method. However, indirect shear contribution of FRP such as the enhancement of aggregate interlock on the shear crack surface is not considered explicitly in Eq.1. The FRP shear contribution in Eq.1 is indeed a total shear force containing both direct and indirect shear contributions. As a result, models of this kind can hardly reveal the nature of this problem and size effect may also exist in the prediction of these models. Best fitting curves based on 35 beam tests (Lu, 2004) for the relationships between predicted FRP shear contributions and tests with different models are shown in Figure 1. The figure clearly shows that lower predictions appear in larger beams, which indicates a size effect on shear contribution of FRP sheets externally bonded to RC beams which is contrary to that of RC beams with or without shear reinforcement.

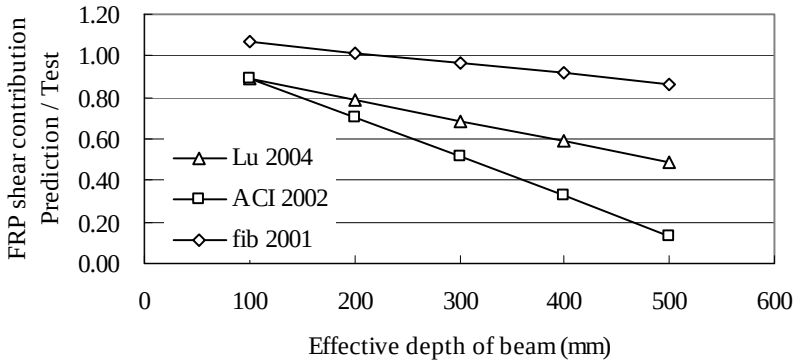

Figure 1 Size effect on shear contribution of FRP sheets

In this paper, the shear contribution of FRP sheets is examined in depth with the assistance of a test program. An improved finite element model is proposed to predict the direct shear contribution of FRP which shows good agreement with the test results in this study and little size effect. More studies are still needed for the indirect shear contribution of FRP.

TEST SPECIMENS AND PROCEDURE

Three RC beams strengthened with FRP U-jackets, which were 3D geometrically similar, were tested. Three corresponding control beams without strengthening were also tested. In order to study the size effect in the shear strength, the span and thickness of the beam, as well as the width, space and thickness of FRP U-jackets, were increased proportionally with the height of the beams, so that all strengthened beams had the same FRP reinforced ratios ρ_f . No steel stirrups were installed in the test span whilst sufficient stirrups were installed in the other span to avoid unexpected failure. All specimens had the same flexural reinforcement ratio. Some important parameters of the beams are listed in Figure 2 and Table 1.

The flexural reinforcing bars were cold drawn deformed steel bars with yield strength of 400MPa. The ends of the flexural rebars in each beam were welded to each other with two layers of short steel bars to avoid anchorage failure.

The nominal span-to-depth ratio λ was 2.0 for all the beams. Here the shear span equals to the distance from loaded points to the centre of support. However, due to the relative large stiffness of backing strips at the loaded points and supported points, it was believed that the real shear span-to-depth ratio λ_r was 1.51, in which the shear span equals to the distance from the edge of loaded backing strip to the edge of supported backing strip.

All the beams were cast in plywood mould from a single batch of concrete and were cured under the same condition for six days before the mould were stripped. The maximum aggregate size was about 30mm. The ages at which the beams were tested vary from 40 days to 90 days. The concrete strength of different beams, together with their shear strengths, are listed in Table 1.

The thickness of CFRP strips is 0.111mm per-layer, with a Young's modulus E_f of 235GPa and tensile strength f_f of 3550MPa.

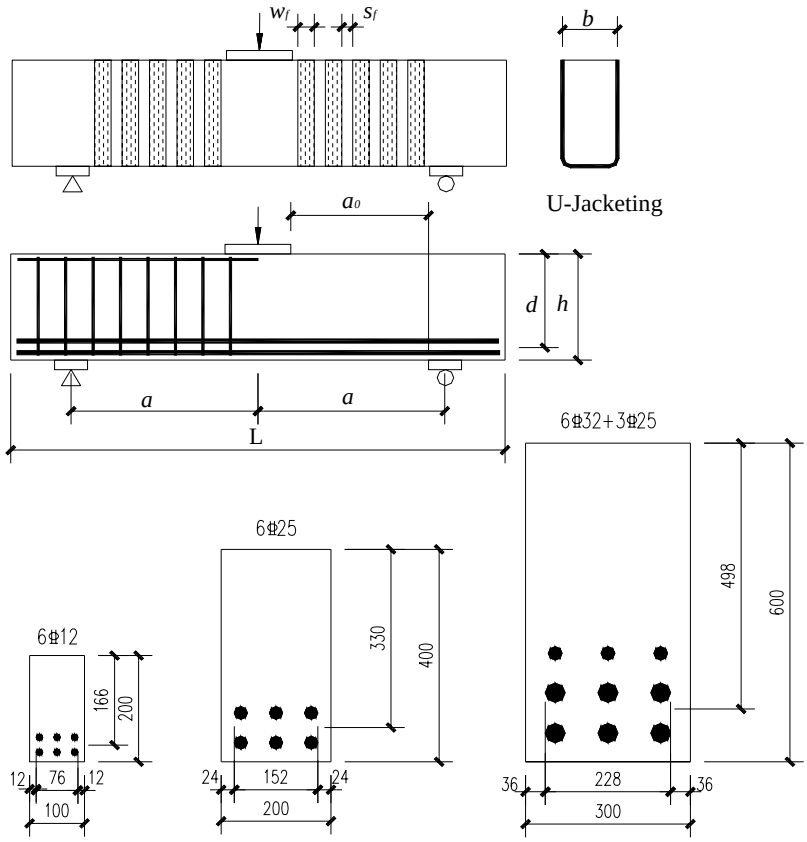

Figure 2 Configurations of specimens

Table1 Basic design parameters and major test results of specimens

Beam No.	RC1	RC2	RC3	U4	U5	U6
Width b (mm)	100	200	300	100	200	300
Height h (mm)	200	400	600	200	400	600
Effective depth d (mm)	166	330	498	166	330	498
Shear Span a (mm)	340	680	1020	340	680	1020
Shear Span a_0 (mm)	250	500	750	250	500	750
Steel reinforcement ratio ρ（%）	4.1	4.5	4.2	4.1	4.5	4.2
Width of FRP strips w_f(mm)				30	60	90
FRP effective thickness t_f(mm)				0.111	0.222	0.333
Central spacing of FRP strips s_f(mm)				50	100	150
Concrete compressive strength f_{cu} (MPa)	51.2	49.7	50.5	51.2	51.2	51.0
Concrete tensile strength f_{ts} (MPa)	2.55	2.93	3.16	2.55	2.93	3.16
Concrete Young's Modulus E_c (MPa)				34272		
Shear capacity of beam P (kN)	159.4	709.1*	1626.0	202.7	809.3	2017.9

* Specimen RC2 failed at the span with stirrups.

TEST RESULTS AND DISCUSSIONS

Components of the shear contribution of FRP sheets

Generally the shear strength of FRP strengthened RC beam consists of two components which are shear contribution of RC beam V_{RC}, and shear contribution of FRP V_f. Detailed research (Ye *et al*. 2002) has shown that the shear contribution of FRP V_f can be further divided into two portions, which are referred as the direct contribution V_{fd} and indirect contribution V_{fi}, respectively. The direct shear contribution V_{fd} is relatively easy to be understood which equals to the total tension of FRP strips. The indirect shear contribution V_{fi} represents all the other shear strength enhancements with FRP strengthening, such as the change of shear crack angle, enhanced aggregate interlock and reduction of damage concentration. As a result, the shear strength of an FRP strengthened RC beam can be presented as Eq. 2.

$$V = V_{RC} + V_f \quad (2a)$$

$$V_f = V_{fd} + V_{fi} \quad (2b)$$

where V is the shear strength of the FRP strengthened RC beam;

V_{RC} is the shear contribution of the reinforced concrete beam;

V_f is the shear contribution of FRP sheets externally bonded on the web;

V_{fd} is the direct shear contribution of FRP, which equals the total FRP tensile force.

V_{fi} is the indirect shear contribution of FRP, which represents the sum of all the other influences of FRP on the beam.

Most existing models ignore V_{fi} for simplicity. However, V_{fi} may play an important role when estimating the overall shear contribution of FRP sheets. Figure 2 shows the development of FRP direct shear contribution ratio V_{fd}/V for the three specimens. Here V_{fd} equal the summation of FRP tensile forces calculated from the measured FRP strains. This ratio increases with the decrease of the beam height. The sum of FRP tensions suddenly drops when an FRP strip detaches from the concrete. The released forces from the detached FRP strip are transferred to other components of the beam, such as the steel reinforcement or the concrete. Since the total loading is still increasing without any sudden change, the sudden drop of FRP direct contribution means a sudden increase to the FRP indirect shear contribution V_{fi}. Another phenomenon in Figure 2 is that larger beams take a longer period from the first FRP strip separation to the ultimate state, which indicates that the larger the beam, the more important the V_{fi} is.

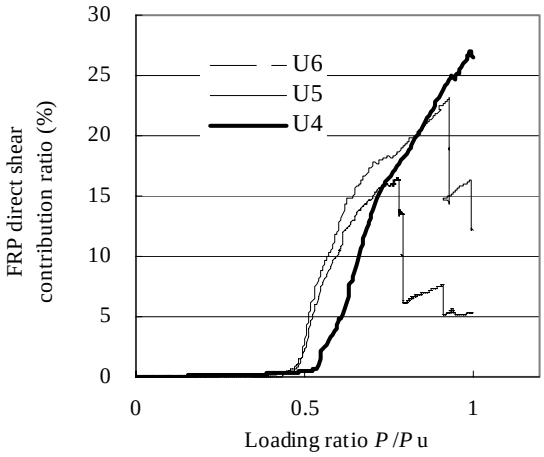

Figure 2 Development of the direct shear contribution of FRP sheets

The direct shear contribution of FRP sheets V_{fd}

Comparison between V_{fd} and the strength of direct-pull tests

The major function of FRP sheets before failure is to provide tensions to resist the shear force. The loading condition of FRP U-jackets externally bonded on the beam is similar to that of FRP sheets in a direct-pull test as shown in Figure 3. The summation of these tensions is equal to V_{fd}, whose maximum value is generally reached just before the first FRP sheet fails due to debonding. The interaction between different FRP sheets is quite weak and it may be ignored before V_{fd} reaches its maximum value. The major difference between FRP externally bonded on the side in shear and FRP in a direct-pull test is the concrete stress state underneath the FRP sheets.

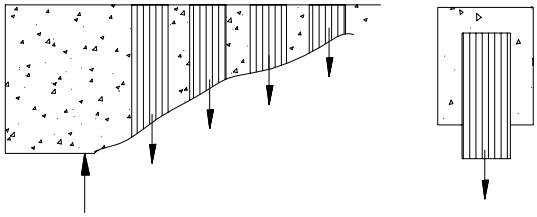

(a) FRP externally bonded on the web in shear (b) Direct-pull test

Figure 3 Loading condition of FRP sheets

In the direct-pull test, the concrete underneath the FRP is basically in a pure shear stress state. For FRP sheets bonded on the side of a beam, besides the FRP-to-concrete interfacial stresses, the concrete is part of the strut of the beam which carries a compressive stress approximately parallel to the diagonal crack and a tensile stress perpendicular to the compressive stress. So the stress state is much more complex and the strut stress may reduce the FRP-to-concrete interfacial strength, which results in a reduction of effective FRP debonding strain.

Reduction of concrete tension strength f_t

Lu (2004) established his FRP shear contribution model by combining his bond-slip relationship and simplified diagonal crack models, in which the bond-slip relationship is obtained from direct-pull tests. According to the aforementioned comparison, the FRP-to-concrete interfacial strength needs to be reduced when such bond-slip relationship is applied to FRP-to-concrete interface in shear strengthening. The concrete tensile strength f_t is critical for the FRP-to-concrete interfacial strength, since the debonding mode is due to the cracking of the concrete underneath the FRP sheets.

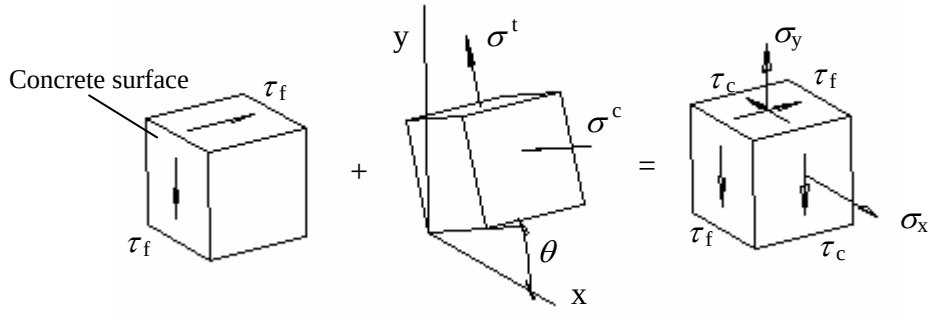

State A
Pure shear state in a direct-pull test

State B
Biaxial stress state in the strut of the beam

State C
Triaxial stress state in the strut underneath an FRP sheet

Figure 4 Superposition of stress states of concrete in the strut underneath the FRP sheets

Figure 4 demonstrates different stress states of concrete and their superposition. Experimental observation also finds that the FRP debonding failure and RC beam shear failure are very close to each other, though they do not happen at the same time. Thus, the two stress state components (State A and B in Figure 4) in the concrete strut underneath the FRP can be assumed to have reached their ultimate states when debonding failure happens. In the pure shear state (State A), the shear stress τ_f is assumed to be equal to the peak average bond stress τ_{ave} (Eq.3), (Lu *et al*. 2005b). The biaxial stress state (State B) when strut fails is debatable. Different researchers give different definitions. In this study, the compressive stress in the strut at failure is assumed to equal to $0.85f_c'$ (Eq.4) (Alshegeir & Ramires 1990). The tensile strain of the strut at failure is assumed to be twice the concrete peak tensile strain $\varepsilon_{t,p}$, because some tiny but visible shear cracks are found in concrete underneath the FRP above the critical diagonal crack. If $\varepsilon_{t,p}$ is calculated from Eq.5 (Guo 1997), the corresponding tensile stress of the strut can be found from Eq.6 (Belarbi & Hsu,1994).

$$\tau_f = 0.59 f_t^{1.25} \sqrt{\frac{2.25 - w_f / s_f}{1.25 + w_f / s_f}} \tag{3}$$

$$\sigma_c = 0.85 f_c' \tag{4}$$

$$\varepsilon_t = 2\varepsilon_{t,p} = 2 \times 65 \times 10^{-6} f_t^{0.54} \tag{5}$$

$$\sigma_t = \frac{0.31\sqrt{f_c'}}{(12500\varepsilon_t)^{0.4}} \tag{6}$$

where f_c' equals to $0.8f_{cu}$, w_f is the width of the FRP sheets, s_f is the central spacing of FRP sheets.

In State B of Figure 4, θ is the average diagonal crack angle which equals 33^o for the strengthened specimens in this study.

A coordinate system transformation is needed to transform the biaxial stress of the strut σ_c and σ_t to the global coordinate system σ_x, σ_y and τ_c, while τ_f in State A does not need any change. So the stress tensor in State C under global coordinate system can be given as Eq.7.

$$\sigma = \begin{bmatrix} \sigma_x & -\tau_c & 0 \\ -\tau_c & \sigma_y & -\tau_f \\ 0 & -\tau_f & 0 \end{bmatrix} \quad (7)$$

A reduced tensile strength of concrete f_t' can be finally obtained for the triaixial stress state in Eq. 7 following the failure criterion proposed by the Chinese Academy of Building Research (2002) and Guo (2003):

$$f_t' = r \cdot \frac{-0.96 f_t f_c}{f_t - (0.048 + 0.96r) f_c} \quad (8a)$$

$$r = \sigma_1 / \sigma_3 \quad and \quad r \le -0.05 \quad (8b)$$

where f_t' is reduced concrete tensile strength, which will be used in the following finite element analysis;

σ_1 and σ_3 are the major and minor principal stress, respectively;

f_t and f_c are the tensile and compressive strength of concrete, respectively.

The reduced concrete tensile strengths of the three specimens are listed in Table 2, compared with their original tensile strengths.

Table 2 Tensile strength of concrete (MPa)

	U4	U5	U6
Reduced tensile strength f_t'	2.12	2.25	2.34
Tensile strength f_t	2.55	2.93	3.16

Finite element analysis

The upper half of the critical FRP that may be separated from the beam was modelled with the truss-spring model as in Lu *et al.* (2005a) (Figure 5). The FRP sheets are simulated using a series of truss elements for simplicity. Each node of the truss elements is connected to the concrete surface with a nonlinear spring element. A pre-defined slip field is applied at the end of the FRP sheets to simulate the opening of the diagonal crack. The properties of the spring were calculated based on the FRP-to-concrete interface bond-slip relationship proposed by Lu *et al*. (2005b) using the reduced concrete tensile strength f_t' instead of f_t. Three different simplified diagonal crack models are presented by Lu *et al* (2005a) as shown in Figure 6. For each diagonal crack model, there is a corresponding slip field. Each slip field is applied to the finite element model for the largest specimen U6. Figure 7 compares the FRP tensile strain distributions before debonding along the diagonal crack obtained from different slip fields. It can be seen that Crack model A gives the closest agreement with the test result due to sufficient flexural reinforcement which limits the cracking opening at the bottom of the beam. Crack model A will be adopted in the following calculations.

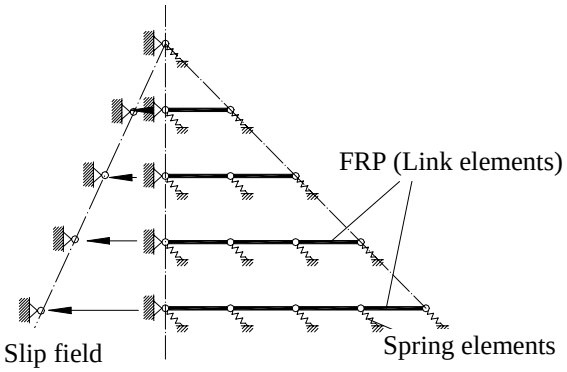

Figure 5 Simplified FE model for externally bonded FRP U-jackets on RC beam

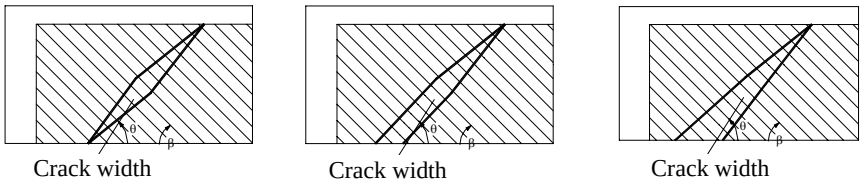

(a) Model A (b) Model B (c) Model C

Figure 6 Simplified diagonal crack models by Lu *et al*. (2005a)

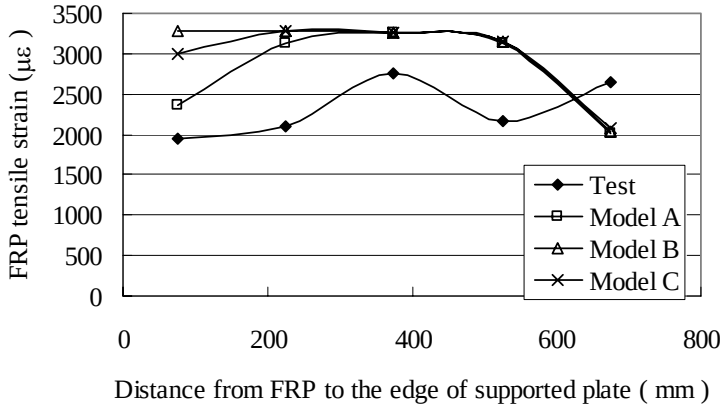

Figure 7 FRP strain distribution for different diagonal crack models: specimen U6

As aforementioned, the maximum value of V_{fd} is reached before the first FRP sheet completely debonds and V_{fd} is equal to the sum of tensions provided by FRP sheets along the diagonal crack. As an elastic material, the tension in FRP is equal to the product of the tensile strain and the Young's modulus of FRP. So the distribution of FRP tensile strain along the diagonal crack is directly related to V_{fd}. The average tensile strain of FRP sheets when V_{fd} reaches its maximum value is called FRP average peak strain. Finite element analyses were carried out for all the three specimens and Figure 8 compares the calculated distributions of FRP tensile strain before the first FRP sheets fails along the diagonal cracks with the test results. The simulation gives satisfying results.

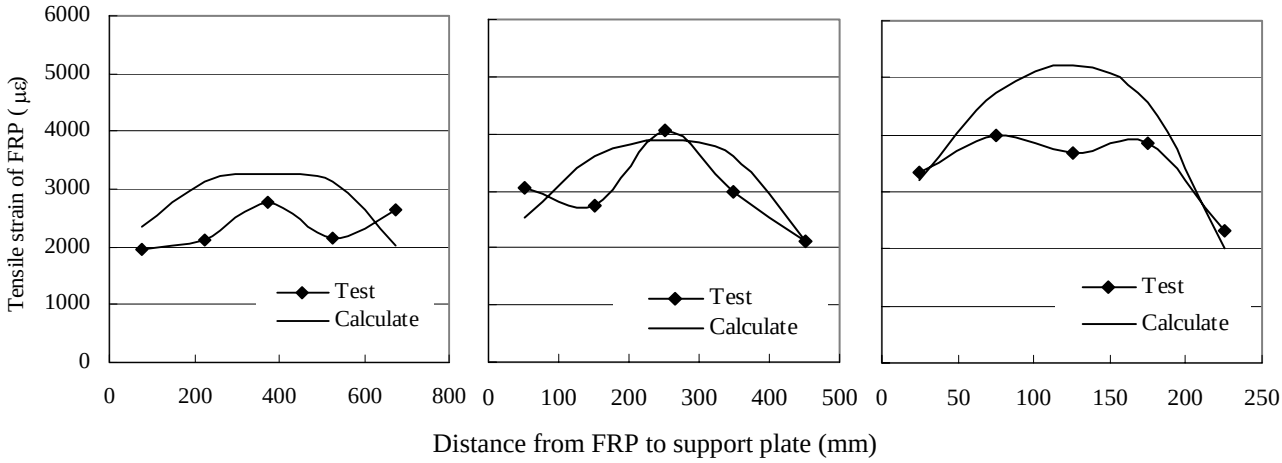

(a) U6 h=600mm (b) U5 h=400mm (c) U4 h=200mm

Figure 8 Measured FRP strain distribution along the diagonal crack versus FE prediction

Figure 9 compares the FRP peak average strains of different specimens obtained by tests and some existing models. The finite element model adopted in this study is the same as the one used in Lu *et al*. (2005a) except that the reduced concrete tensile strength was used here. Lu *et al*'s model (2005a) obviously overestimates the direct contribution of FRP from Figure 9. The results of all other models are also much larger than that of the present finite element analysis, mainly because all these models take the indirect shear contribution of FRP sheets V_{fi} as part of direct portion V_{fd}.

It should be mentioned that in this test program, the tension-compression strength ratio of the concrete is much lower than most empirical formulas. For example, U4 has a cubic strength of 51.2MPa but a tensile strength of 2.55MPa. This tensile strength is smaller than the value calculated from the empirical formulas proposed by the Chinese code in which f_t can be found from f_{cu} to be 3.44MPa. As a result, Chen and Teng's model (2003b) which is based on the compressive strength of concrete for convenience of practical design gives worse prediction than Lu *et al*'s model (2005a) which is based on the tensile strength of concrete. It also implies that the interfacial debonding is mainly governed by the tensile strength of concrete underneath FRP, which was discussed in detail in Lu *et al*. (2005b).

The peak FRP average strain decreases as the height of beam increases for the test specimens. Note that the thickness of FRP is proportional to the beam height. The FE predictions give a satisfying prediction of this trend. Most existing models such as Lu *et al* (2005a), Chen & Teng (2003b), ACI 440 (2002) also demonstrated similar trends despite over estimating the peak strains. Since the descending trend of FRP peak average strain can be predicted with satisfactory accuracy, little size effect exists on the direct shear contribution of FRP sheets V_{fd} especially when it is predicted with the reduced f_t as proposed in this study. So the size effect on the FRP shear contribution mainly comes from the indirect shear contribution V_{fi}.

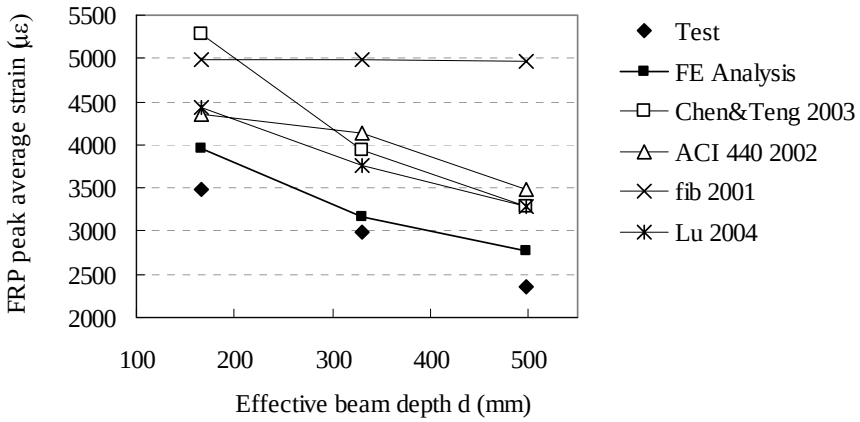

Figure 9 The peak average strains of FRP sheets

The indirect shear contribution of FRP sheets V_{fi}

Apart from tension forces which directly resist the shear force, the FRP sheets have many other effects on the mechanical behaviour of the reinforced concrete beam. These effects are considered as the indirect shear contribution V_{fi}, which is very complicated and can hardly be obtained directly from tests. However, some concepts are discussed as follows.

Firstly, the inclination angle of diagonal crack decreases after the beam being strengthened by FRP U-jackets as shown in Figure 10. This results in a larger uncracked concrete region near the loaded point which enhances the loading capacity of the uncracked concrete and flexural compression zone.

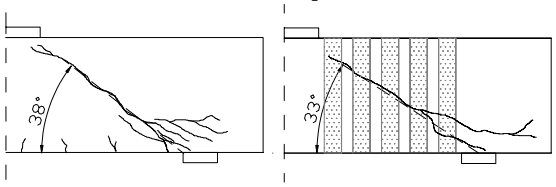

(a) RC1 (b) U4

Figure 10 Diagonal cracks in RC1 and U4 at failure

Secondly, the FRP sheets externally bonded on the side resist the opening of the diagonal crack, which in turn enhance the crack-surface shear retention and increase the residual tensile stresses across the cracks. Figure 11 shows the distribution of the principal tensile strain in RC3 and U6 obtained from photogrammetry. The larger the tensile strain, the darker it is on the figure. An obvious diagonally cracked region is seen in RC3 (Figure 11a) while the tensile strain in the diagonal cracked region in U6 is relatively small (Figure 11b), indicating a smaller crack width.

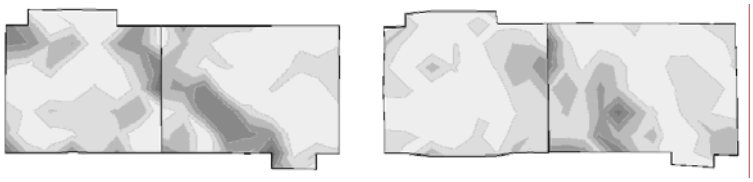

(a) RC3 (b) U6

Figure 11 Principle tensile strain distributions on the webs of RC3 and U6 at a load of $P \approx 0.75/P_u$

Also, the dowel action plays a more important role in FRP strengthened RC beam since the concrete supporting the flexure steel bars is enhanced by FRP sheets and it is believed that most of the forces released by FRP failure are carried by dowel action.

As the components are similar, the indirect shear contribution V_{fi} may be simulated by the shear strength of an equivalent RC beam without web reinforcement, i.e. the size effect on V_{fi} may be converted to the size effect on RC beam without web reinforcement.

CONCLUSIONS

1. The shear strength of FRP strengthened RC beams may be divided into three components, the shear contribution of RC beams, the direct shear contribution of FRP sheets and the indirect contribution of FRP sheets.
2. The direct shear contribution of FRP sheets is equivalent to the load capacity of a direct-pull test, where the concrete tensile strength f_t has to be reduced to consider the different stress states of the concrete underneath the FRP.
3. The direct shear contribution of FRP sheets shows little size effect.

ACKNOWLEDGMENTS

The authors would like to thank Dr J.F. Chen and Professor J.M. Rotter of Edinburgh University, UK for their contributions in the experimental design, discussions and writing of the paper. They would also like to acknowledge the financial supports provided by the Natural Science Foundation of China (National Key Project No. 50238030), the Royal Society through Royal Society-NSFC China-UK Joint Project (Grant No. IS 16657) and the Research Grants Council of the Hong Kong Special Administrative Region, China (Project No: PolyU 5151/03E).

REFERENCES

ACI 440 (2002). *ACI 440.2R-02 Guide for the design and construction of externally bonded FRP systems for strengthening concrete structures*.

Alshegeir, A. and Ramires, J. A. (1990). "Analysis of disturbed regions with strut-and-tie models". *Structure Engineering Rep. No. CE-STR-90-1*, Purdue University, West Lafayette, India.

Belarbi, A. and Hsu, T. T. C. (1994). "Constitutive laws of concrete in tension and reinforcing bars stiffened by concrete", *ACI Structual Journal*, 91(4), 465-474

Chen, J. F. and Teng, J. G. (2003a). "Shear capacity of FRP-strengthened RC beams: FRP debonding", *Construction and Building Maerials*, 129(5), 615-625.

Chen, J.F. and Teng, J.G. (2003b). "Shear capacity of FRP strengthened RC beams: fibre reinforced polymer rupture", *Journal of Structural Engineering*, ASCE, 129(5), 615-625.

China Academy of Building Research, (2002). "Code for design of concrete structures". China Architecture and Building Press, Beijing, China, 93-98

fib (2001). "Externally bonded FRP reinforcement for RC structures".

Guo, Z. H. (1997). "The strength and deformation of concrete (Experimental foundation and constitutive law)", Tsinghua Univ. Press, Beijing, China.

Guo, Z. H., Shi, X. D.,(2003). "Priciples and analysis of reinforced concrete". Tsinghua Univ. Press, Beijing, China, 24-32

Lu, X. Z. (2004). "Studies on FRP-concrete interface". *PhD Thesis*, Tsinghua University, Beijing, China.

Lu, X. Z., Chen J. F., Ye L. P., Teng J. G., Rotter J. M., (2005a). "Theoretical analysis of FRP stress distribution in U jacketed RC beams", *Proc. 3rd Int. Conference on Composites in Construction (CCC2005)*, Lyon, France, July, 2005, 541-548.

Lu X. Z., Teng JG., Ye L.P., Jiang J.J., (2005b). "Bond-slip models for FRP sheets/plates externally bonded to concrete". *Engineering Structures*. 27(6), 938-950. .

Ye L. P., Yue Q. R., Zhao S. H., Li Q. W., (2002). "Shear strength of reinforced concrete columns strengthened with carbon-fiber-reinforced plastic sheet", *Journal of Structural Engineering, ASCE.*, 128 (12), 1527-1534.